

# Using Sequence Alignments to Predict Protein Structure and Stability With High Accuracy

Alan Lapedes,<sup>1,2,\*</sup> Bertrand Giraud,<sup>3</sup> Christopher Jarzynski<sup>1</sup>

<sup>1</sup>Theoretical Division, Los Alamos National Laboratory

MS B213, Los Alamos N.M. 87545 USA

<sup>2</sup> Santa Fe Institute, 1399 Hyde Park Rd, Santa Fe NM 87501 USA

<sup>3</sup>Service Physique Théorique, DSM, C.E. Saclay 91191 Gif/Yvette, France

\*To whom correspondence should be addressed; E-mail: asl@lanl.gov

We present a sequence-based probabilistic formalism that directly addresses co-operative effects in networks of interacting positions in proteins, providing significantly improved contact prediction, as well as accurate quantitative prediction of free energy changes due to non-additive effects of multiple mutations. In addition to these practical considerations, the agreement of our sequence-based calculations with experimental data for both structure and stability demonstrates a strong relation between the statistical distribution of protein sequences produced by natural evolutionary processes, and the thermodynamic stability of the structures to which these sequences fold.

This manuscript was originally written in 2002 and available from <http://library.lanl.gov/cgi-bin/getfile>. It's being deposited here for greater ease of access.

Our approach is analogous to solving an inverse problem of statistical mechanics: determine the physical interaction parameters of a twenty-state spin system given a set of sequences drawn from the Boltzmann equilibrium distribution. The sequences we consider are sets of aligned protein sequences drawn from variable sequence families defined in the Pfam database [1]. We assume that within each family the sequences adopt a common (but in principle unknown) fold whose underlying structure is reasonably conserved across the family. Each sequence of length  $L$  of a given family can be viewed as a different global state of an  $L$ -site, twenty-state (for twenty amino acids) spin system, with spin-spin (i.e. residue-residue) interactions determined by (1) the (unknown) structure of the associated fold, and (2) the physico-chemical characteristics of the residues. Solving the inverse problem to determine the underlying physical interactions addresses “correlation at a distance”, in which correlations between locally connected sites in an interacting network such as a spin system, or a protein, can propagate throughout the network, leading to observed correlations between sites that have no direct physical interaction [2]. Such propagated correlations can be even greater than correlations between any directly connected sites in the system [3]. Previous computational work on abstract models of proteins [4], as well as a statistical analysis of the frequency of ion-pairs in crystal structures of real proteins [5], provided early hints that Boltzmann-like statistics are associated with aspects of protein architecture. In view of complicated evolutionary pressures acting on naturally evolved protein sequences it is surprising that developing a strictly thermodynamic approach can, as we demonstrate below, lead to an accurate predictive methodology for both protein structure and stability.

Other work relating sequence statistics to physical interactions, but restricted to as-

suming independent (non-interacting) sites, successfully characterized protein-DNA binding interactions given sequence data [6, 7, 8]. “Semi-rational” protein sequence design, see e.g. [9], also assumes independent sites, and analyzes natural sequence variation to suggest mutations leading to greater thermodynamic stability. However, analysis of mutations in sets of aligned sequences, first for RNA sequences [10] and later for protein sequences [11], has shown that mutations in pairs of sequence positions are often correlated. Such pairwise correlations have been used in attempts to predict spatially proximate residues (contacts) in folded proteins [12, 13, 14, 15, 16, 17, 18]. The hypothesis is that pairs of variable residue positions, possibly distant along the sequence but spatially proximate in the folded molecule, will display significant covariation. Published approaches analyze correlations between at most two sequence positions at a time, hence they inherently assume that each potentially interacting pair of positions under consideration is physically isolated from all other positions [19]. This assumption is reasonable for RNA molecules, given the saturating hydrogen bond interaction between base-pairs, and accuracy of contact prediction for RNA using pairwise covariation formulae is relatively high [10]. This assumption is not reasonable for the typically diffuse and networked interactions among amino acids, and accuracy of contact prediction for proteins using pairwise covariation formulae is relatively poor. Pairwise covariation formulae were recently used for a qualitative description of stability changes upon mutations in the SH3 domain, as well as for contact prediction [18]. Attempts to chain together separate pairwise analyses to approximate interaction networks in proteins [21] can be illuminating, suggesting that a complete formalism to address network effects would be fruitful.

The Boltzmann network method presented here does not treat each individual pair of sites of interest as isolated from other residues. Instead, we construct a probability distribution describing full length sequences of length  $L$  for each protein sequence family.

Any given sequence alignment typically contains enough data to estimate only single and pairwise amino acid frequencies with reasonable accuracy. One point of departure from previous analyses using single and pairwise frequencies is that we adopt an information theoretic viewpoint, and ask for the least biased probability distribution, *defined over all  $L$  sites*, whose first and second order moments match the single and pairwise amino acid frequencies of the given data. “Least biased” is defined to be the maximum entropy distribution [20], which in our context may be intuitively viewed as the flattest distribution among the many distributions that have first and second order moments matching the amino acid frequencies in the given data [22].

The maximum entropy distribution whose moments match a given set of single and pairwise amino acid frequencies may be written in the following form [23], reminiscent of thermal Boltzmann statistics

$$P(X) = \frac{\exp[-E(X)]}{Z}, \quad (1)$$

where  $E$  is a sum of single and pairwise interactions among potentially all amino acids

$$E(X) = \sum_{\alpha\beta ij} \lambda_{ij}^{\alpha\beta} x_i^\alpha x_j^\beta + \sum_{\alpha i} \lambda_i^\alpha x_i^\alpha. \quad (2)$$

$x_i^\alpha$  denotes the residue present at position  $i$  in sequence  $X$ , it has the value 1 if amino acid  $\alpha$  is present at sequence position  $i$ , and is 0 otherwise. The  $\lambda$ 's are adjustable parameters (to be determined) such that the calculated first and second order moments of this distribution match the single and pairwise amino acid frequencies in the given sequence alignment.  $i$  and  $j$  label sequence positions (1 to  $L$ ), and  $\alpha$  and  $\beta$  label the twenty possible amino acids.  $Z$  is a normalization factor. It can be shown [25] that matching the moments of the maximum entropy distribution to the given sequence data is equivalent to maximizing the loglikelihood of the given sequence data given the parametric form, Eqns. (1,2), for

the probability distribution. This formalism is related to Boltzmann Machines [27] and Graphical Models [28], used in other contexts.

So far,  $E$  is merely a suggestive symbol appearing in a probability distribution, Eqns. (1,2), describing sequence statistics of an alignment. However, it is shown below if the  $\lambda$ 's are adjusted so that the moments of the distribution match the given amino acid frequencies, then  $E$  is highly correlated with a real, physical, thermodynamic free energy of unfolding. Furthermore, we use the probability distribution over all  $L$  sites, Eqns. (1,2), to resolve issues of correlation at a distance (network effects) in proteins, resulting in significantly improved contact prediction from sequence information.

We consider aligned sequences for eleven domains [29] taken from the Pfam [1] database, with associated x-ray crystal structures taken from the Protein Data Bank[30]. These domains were chosen to be diverse in sequence (less than 50% pairwise sequence identity) and to have more than 200 sequences per family. The distance between a pair of residues was defined to be the distance between their carbon  $\beta$  atoms, and pairs of residues with carbon  $\beta$  distance of less than 7 Angstroms were defined to be in contact (carbon  $\alpha$  coordinates were used for glycines). Results reported below are robust to changes in definition of contact.

Prediction of which residues are directly interacting (i.e. in physical contact) uses the concept of conditional mutual information [20] applied to  $P(X)$  after the  $\lambda$ 's have been determined for each sequence family. In our context, conditional mutual information,  $CMI$ , measures the degree of covariation between residues at sequence positions  $i$  and  $j$  that is solely due to direct effects of  $i$  on  $j$  (and *vice versa*), factoring out contributions to the correlation between  $i$  and  $j$  caused by interaction of both  $i$  and  $j$  with the rest of the network of residues. It is a discrete (and nonlinear) analogue of linear partial correlation analysis [31, 32] and is intuitively described by this process: (a) freeze all residues other

than those at  $i$  and  $j$  to a fixed state, thus preventing information propagation through the rest of the network, (b) calculate the mutual information between  $i$  and  $j$ , using  $P(X)$ , above, with the rest of the network frozen, and (c) average this result over all possible frozen states of the rest of the network [33]. Pairs of sites with high  $CMI$  (over a user defined threshold) are predicted to be in contact.

Two quantities, specificity and sensitivity, are typically used to characterize predictive ability. Specificity is defined as the fraction of predicted contacts that are actual contacts (as defined by carbon  $\beta$  distances) i.e. the overall probability that a predicted contact is correct. Sensitivity is defined as the fraction of actual contacts that are correctly predicted. High specificity is more desirable than high sensitivity, because in our context predicting even a small number of contacts with high accuracy provides extremely valuable constraints on *ab initio* protein structure calculations [34, 35]. Hereafter we refer to specificity as “accuracy”. To survey accuracy as a function of  $CMI$  threshold we successively lowered the  $CMI$  threshold, in effect walking down a list of predicted contact pairs ordered by  $CMI$  value, for each domain. This process yields accuracy of prediction as a function of the number of pairs predicted to be in contact [36].

To compare our method to others we also analyzed contact prediction accuracy using (a) a pairwise covariation measure [18] (denoted as  $\Phi AM$  for  $\Phi$  Association Method [37], which we believe to be the most accurate of published methods), (b) conventional pairwise mutual information [19] (denoted as  $MI$ ) and (c) a baseline reference resulting from random selection of position pairs (denoted as *Random*). The measure used in (a) above also incorporates some correction for phylogenetic artifacts. Fig. (1) shows overlaid curves for accuracy of contact prediction via the different methods, versus number of predicted contacts, for the SH3 domain. The most accurate method is the Boltzmann network method, which uses conditional mutual information to predict contact pairs. Accuracy

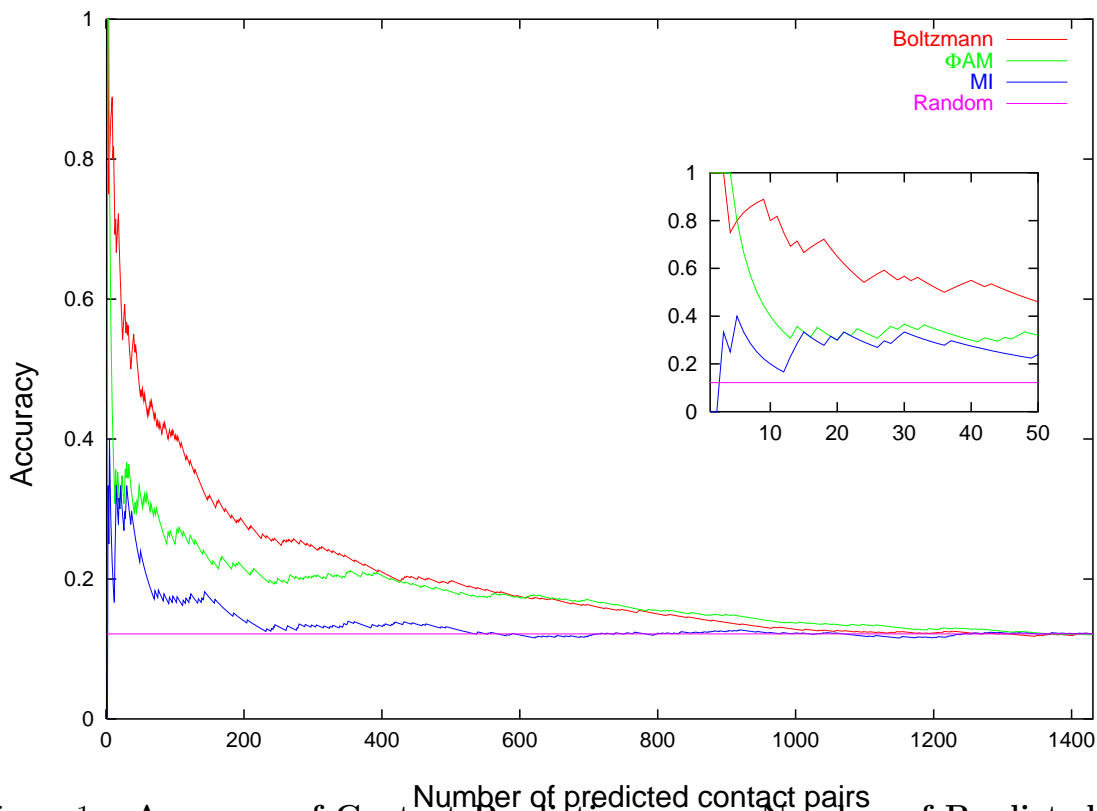


Figure 1: **Accuracy of Contact Prediction versus Number of Predicted Contacts:** Accuracy of prediction (y-axis) vs. number of predicted contact pairs (x-axis) for the SH3 domain is shown. *Boltzmann*, the top curve, is the result of the Boltzmann network method.  $\Phi AM$  is the result of what we believe to be the most accurate published pairwise covariation method [18] (does not address network interactions, does address phylogenetic artifacts), *MI* is the result of pairwise mutual information (does not address network interactions), and *Random* is the average result of picking at random a specified number of contacts. The inset blows up the region from 1 to 50 predicted contacts. The accuracy of contact prediction using the Boltzmann network method, which incorporates co-operative effects among residues, significantly exceeds that of other methods.

varies somewhat from family to family, therefore we show the averaged accuracy over eleven domains in Fig. (2) using the same four predictive methods. The Boltzmann network method has on average consistently higher accuracy for a greater number of predicted contacts. Predicted contacts for the eleven domains using the Boltzmann network method are available in the supplemental material [38].

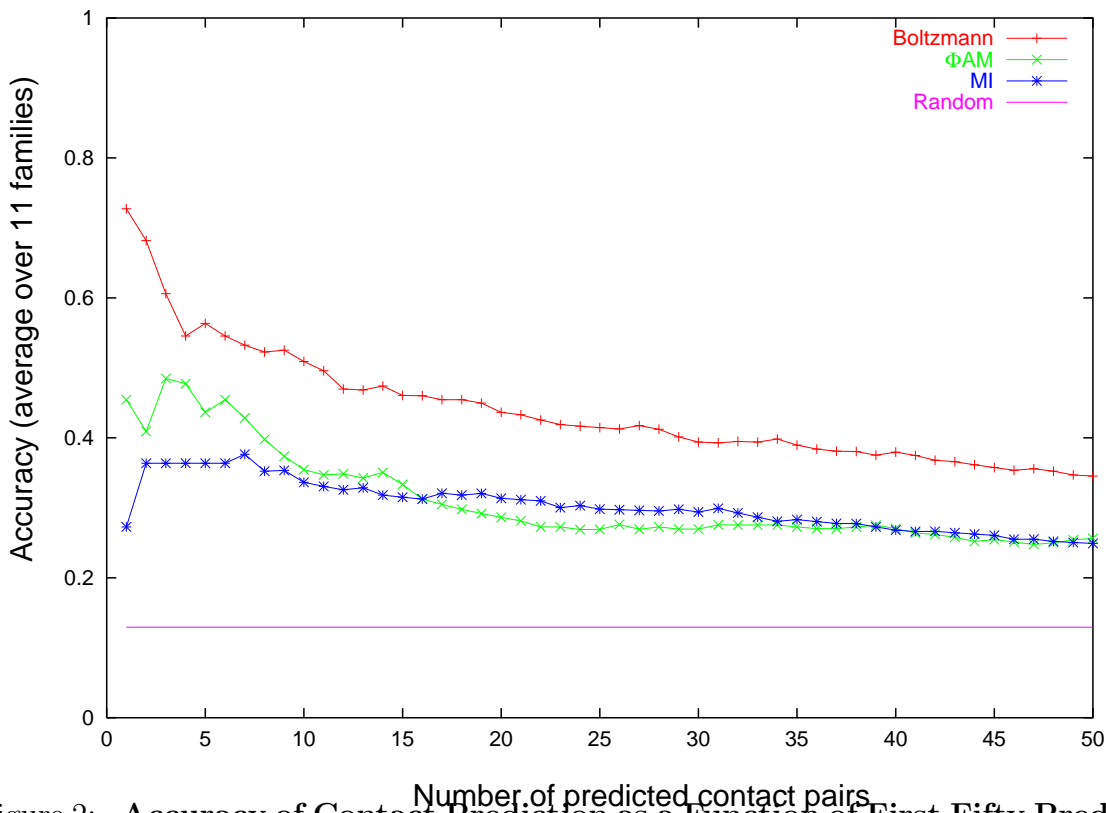


Figure 2: **Accuracy of Contact Prediction as a Function of First Fifty Predicted Contacts:** An Average over eleven domain families, for the same predictive methods of Fig. (1). *Boltzmann*, the top curve, is the result of the Boltzmann network method presented here and has significantly higher average accuracy, demonstrating the importance of addressing co-operative effects within proteins.

The maximum entropy probability distribution, Eqn. (1), has a thermal, Boltzmann form with exponent  $E(X)$ . After the  $\lambda$ 's have been determined for a given sequence alignment,  $E(X)$  assigns an “energy” value to any sequence  $X$ . Interpreting  $E(X)$  as



an effective free energy relative to the unfolded state allows a free energy of unfolding [39],  $\Delta G = -E(X)$ , to be predicted using our formalism. Changes in sequence,  $X$ , will change  $E(X)$  and hence the  $\Delta G$  of sequence mutants can be calculated and compared to experiment. Experimentally determined melting temperatures (assumed proportional to the free energy of unfolding) for wildtype Fyn SH3 sequence, and for a set of single, double and triple mutants of the wildtype were reported in [18]. To assess how well co-operative non-additive effects are captured by our formalism, we calculated  $\Delta G$  values after the  $\lambda$ 's had been determined in two different ways: (1) the interaction parameters,  $\lambda_{ij}^{\alpha\beta}$ , were allowed to adjust during the determination of the probability distribution  $P(X)$ , (2) the interaction parameters,  $\lambda_{ij}^{\alpha\beta}$ , were held fixed to zero, allowing only additive effects to be captured by the remaining adjustable single site  $\lambda_i^\alpha$  parameters [40]. As will be seen below, the correct prediction of the effects of even single site mutants requires consideration of the other sites with which it interacts. The eleven residues identified by a structural analysis [18] to be in the hydrophobic core of the SH3 domain were selected for use in assessing  $\Delta G$  prediction, i.e. the  $\lambda$  parameters used for computing  $\Delta G$  allowed potential interaction among all eleven sites of the hydrophobic core. Significant sequence variation is necessary input information for our method, and so within this set of eleven core positions we report  $\Delta G$  values for mutations involving the three positions (26, 39 and 50 in the numbering scheme of [18]) that displayed the highest mutual information.

Experimentally determined melting temperatures were reported [18] for four single, four double, and three triple mutants, in addition to the wildtype for these three positions. In Fig. (3) the difference of the mutant and wildtype  $\Delta G$ 's as computed by our method for these mutant domains is shown to be highly correlated (absolute value of correlation 0.91) with the experimentally measured melting temperatures. If non-additive and co-operative effects are disallowed by holding the interaction terms to zero then the correlation is poor

(absolute value of correlation 0.02) and the signs of the predicted  $\Delta G$  are incorrect, Fig. (4).

The high correlation of predicted and measured  $\Delta G$  shown in Fig. (3) suggests performing a computational survey of all possible ( $20^3$ ) mutations to search for other interesting single, double and triple mutants. We found no statistically significant prediction of a mutant considerably more stable than wildtype, although the single site mutant F26L has a predicted melting temperature similar to wildtype with a value of 84.9. Predictions of melting temperature for other interesting three site mutants are available in the supplemental material [38]. Results of an extensive computational search among all ( $20^{11}$ ) possible sequences defining a total redesign of the eleven site hydrophobic core of the SH3 domain are also presented [38].

The success of the Boltzmann network formalism in predicting free energy changes upon mutation clearly demonstrates a deep relationship between the statistics of sequences selected by natural evolutionary processes and the thermal stability of the structures to which these sequences fold. However, such a strong relationship would not necessarily be expected given that protein sequences produced by evolution are strongly affected by functional constraints in addition to stability constraints [41]. A possible explanation of the statistics-stability relation is that functional properties are typically confined to localized regions of a protein, e.g. binding sites, and that optimization of small local regions for functional fitness occurs after global selection for sequences that stably fold. An independent, computational investigation of the extent to which sequences are shaped by natural selection for stability was published recently [42] although contact prediction and prediction of free energy changes was not explicitly addressed. In contrast to our sequence based approach, this work used structural information, combined with an all-atom free energy function incorporating a variety of physical effects to computationally

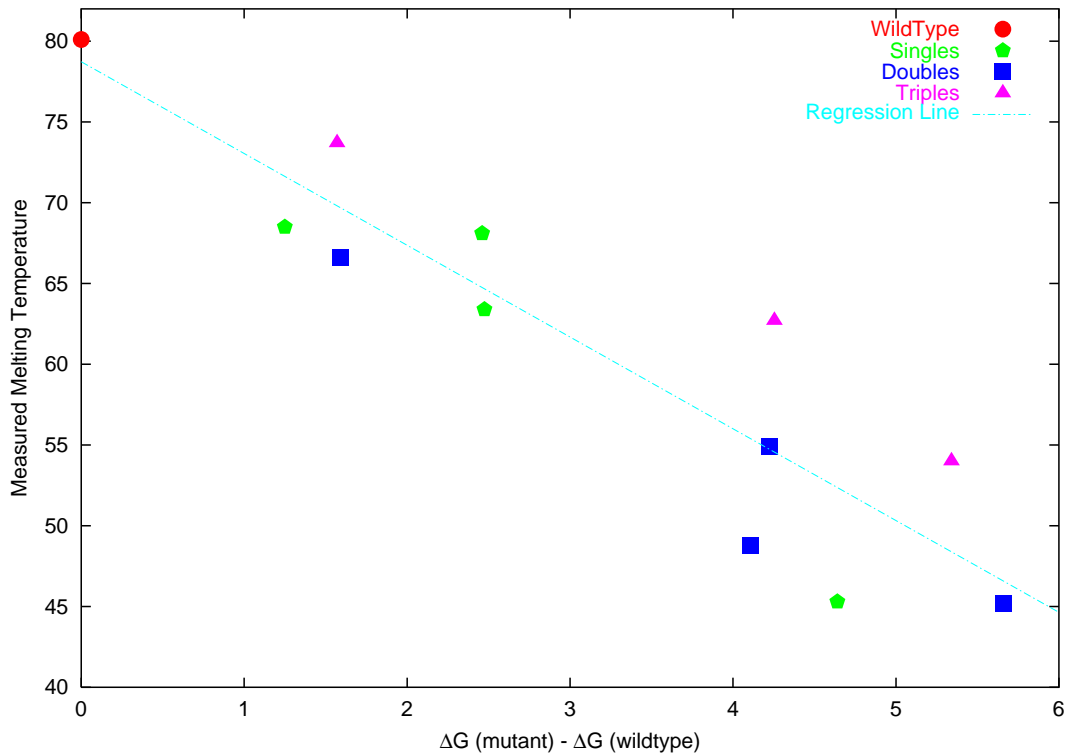


Figure 3: **Measured Melting Temperature versus Predicted Free Energy of Unfolding: Network Interactions Allowed** The free energy of unfolding,  $\Delta G$ , computed using the Boltzmann network method versus experimentally measured melting temperature for eleven mutants of the SH3 domain (four singles, four doubles, three triples) as well as the the wildtype. Co-operative and non-additive effects were allowed, resulting in a good correlation of computation with experiment (absolute value of the correlation is 0.91). The single site mutant, *I50F*, as discussed by Larson, involves mutating to a residue more frequent in the alignment and yet is measured to be quite destabilizing with a measured melting temperature of 45.3. Only if network interactions are allowed is this single site mutant correctly predicted as quite destabilizing. The triple mutant *F26I/A39G/I50F*, with a measured melting temperature of 73.7, involves *I50F* with additional compensatory second site mutations. It is correctly predicted as just mildly destabilizing compared to wildtype only if network interactions are allowed. Comparison of this figure (network interactions included) to Fig. (4) (network interactions excluded), shows in general the importance of network interactions.

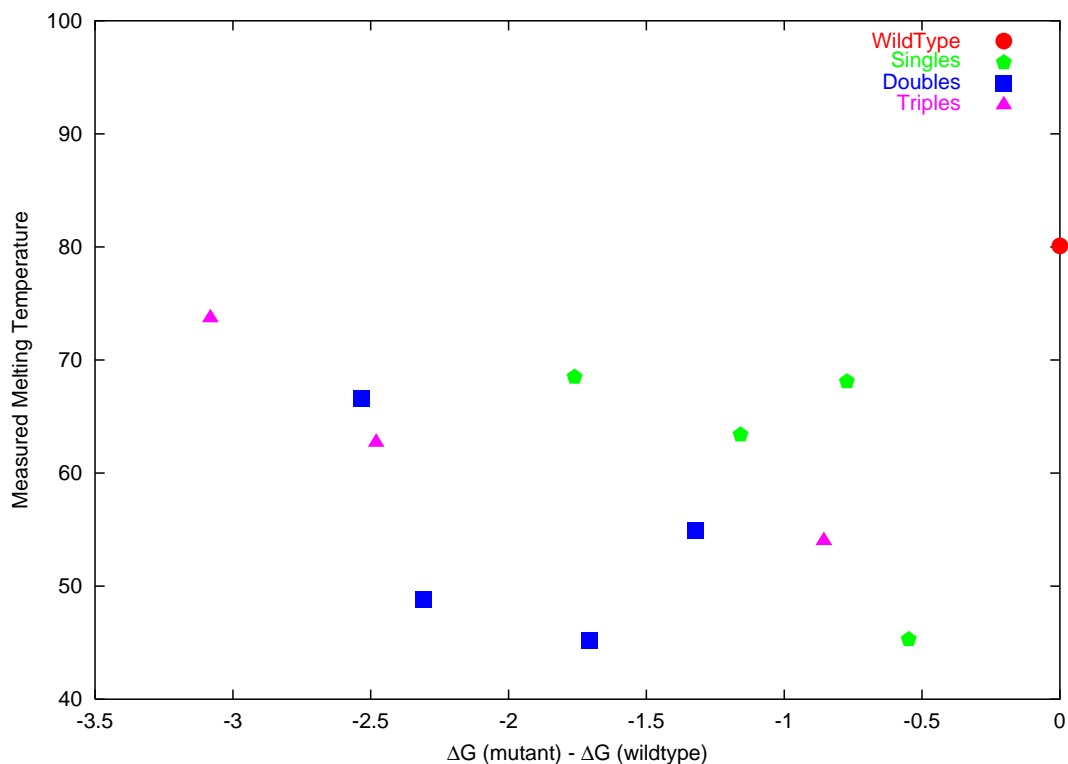


Figure 4: **Measured Melting Temperature versus Predicted Free Energy of Unfolding: Network Interactions Not Allowed** The free energy of unfolding,  $\Delta G$ , versus experimentally measured melting temperature for the same eleven mutants of the SH3 domain and for wildtype, as Fig. (3), but when co-operative and non-additive effects are disallowed by holding the interaction parameters,  $\lambda_{ij}^{\alpha\beta}$ , to zero. There is a dramatic decrease in correlation of computation with experiment (absolute value of the correlation is now 0.01), and even the signs of the stability changes are incorrect when network interactions are disallowed.

design sequences for a variety of domains. The native, naturally occurring sequence for each structure considered was found to be close to optimal for each structure, and for SH3, the pairwise correlations between sites in a set of computationally designed sequences recapitulated the correlations observed in a set of native SH3 core sequences. The extent to which the Boltzmann network's energy function,  $E(X)$ , involving empirical parameters determined solely from sequence information for each domain family, can be identified with the physical/structural effects defining the energy function of this structure-based complementary study remains an interesting issue.

Limiting factors in application of the Boltzmann network algorithm include (1) the amount of naturally evolved sequence data currently available per family (size of the sequence alignment), and (2) the phylogenetic relatedness (and associated selection artifacts) of these sequences. Modifications to the algorithm presented here, e.g. (1) consideration of statistical significance of the fitted  $\lambda$  parameters, and (2) addressing phylogenetic relationships of sequences in an alignment, have the potential to further increase accuracy using naturally evolved sequence sets.

However, the ability to create in the laboratory totally novel sequences for protein domains via artificial evolution techniques such as phage display [43] [44], promises new, rich, and diverse sequence sets with well characterized *in vitro* selection pressures. Such sequence data, when available in greater quantity, and analyzed with the methods herein, offer a new paradigm for sequence based structure prediction, and for the computational design of sequences with preferred properties.

## References and Notes

- [1] E. Sonnhammer, S. Eddy , R. Durbin, *Proteins* **28** pp. 405-420 (1997)

- [2] H. Stanley, *Introduction to Phase Transitions and Critical Phenomena* The International Series of Monographs on Physics Oxford University Press Inc. Oxford and New York (1971)
- [3] B. Giraud, J. Heumann, A. Lapedes, *Phys. Rev. E.* **59**, p. 4983 (1999)
- [4] A. Finkelstein, A. Badretdinov, A. Gutin, *Proteins* **23** pp. 142-150 (1995)
- [5] S. Bryant, C. Lawrence, *Proteins* **9** pp. 108-119 (1991)
- [6] O. Berg, P. von Hippel, *J. Mol. Biol.* **193** pp. 723-750 (1987)
- [7] G. Stormo, *Bioinformatics* **16** pp. 16-23 (2000)
- [8] P. Benos, A. Lapedes, G. Stormo, *Bioessays* **24** pp. 466-475 (2002)
- [9] P. Nikolova, J. Henckel, D. Lane, A. Fersht, *Proc. Natl. Acad. Sci. USA* **95** pp. 14675-14680 (1998)
- [10] R. Gutell, A. Power, G. Hertz, E. Putz and G. Stormo, *Nucl. Acids Res.* **20** pp. 5785-5795 (1992)
- [11] B. Korber, R. Farber, D. Wolpert, A. Lapedes, *Proc. Natl. Acad. Sci. USA* **90** pp. 7176-7180 (1993)
- [12] I. Shindyalov, N. Kolchanov, C. Sander, *Prot. Eng.* **7** pp. 349-358 (1994)
- [13] U. Gobel, C. Sander, R. Schneider, A. Valencia, *Proteins* **18** pp. 309-317 (1994)
- [14] W. Taylor, K. Hatrick, *Prot. Eng.* **7** pp. 341-348 (1994)
- [15] E. Nehe, *Proc. Natl. Acad. Sci. USA* **91** pp.98-102 (1994)
- [16] N. Clarke, *Prot. Sci.* **4** pp. 2269-2278 (1995)

- [17] D. Thomas, G. Casari, C. Sander, *Prot. Eng.* **9** pp. 941-948 (1996)
- [18] S. Larson, A. Di Nardo, A. Davidson, *J. Mol. Biol.* **303** pp. 433-446 (2000)
- [19] Pairwise covariation measures used to date in the literature, such as mutual information [20], are based on the pairwise probability distribution,  $P_{ij}^{\alpha\beta}$ , for amino acid  $\alpha$  to occur at sequence position  $i$  and amino acid  $\beta$  to occur at sequence position  $j$  in an alignment of sequences assumed to fold to a common structure. Mutual information between a pair of positions,  $MI(ij)$ , can be defined in terms of  $P_{ij}^{\alpha\beta}$  as

$$MI(ij) = \sum_{\alpha\beta} P_{ij}^{\alpha\beta} \log P_{ij}^{\alpha\beta} / (P_i^\alpha P_j^\beta)$$

where  $P_i^\alpha$ , respectively  $P_j^\beta$  are the single site distributions at positions  $i$ , respectively  $j$ , determined by appropriate summing over the pair distribution. Other work utilize somewhat different algebraic forms to quantify covariation [21, 18], but ultimately all published methods manipulate probability distributions that involve just two sites at a time, inherently treating each residue pair of interest as physically isolated from all other sites in the system.

- [20] T. Cover, J. Thomas, *Elements of Information Theory* Wiley Series in Telecommunications, John Wiley and Sons (1991)
- [21] S. Lockless, R. Ranganathan, *Science* **286** pp. 295-299 (1999)
- [22] A derivation of the maximum entropy distribution for discrete data (i.e. for amino acids), with application to “toy” (simulated) protein models, can be found in [23]. Independent work invoking maximum entropy principles to describe protein sequences [24] assumed independent sites, and investigated a different set of issues than those considered here.

- [23] A. Lapedes, B. Giraud, L. Liu, G. Stormo, “Correlated Mutations In Models of Protein Sequences: Phylogenetic and Structural Effects” in *Proceedings of the IMS/AMS 1997 International Conference on Statistics in Computational Molecular Biology (Seattle 1997)*, published as Vol 33, Monograph Series of the Inst. for Mathematical Statistics (Hayward Press)
- [24] H. Kono, J. Saven, *J. Mol. Biol.* **306** pp. 607-628(2001)
- [25] Maximizing the likelihood of the given data (a function of the  $\lambda$ 's) by gradient ascent yields the following iterative procedure for successively changing the  $\lambda$ 's by an amount  $\Delta\lambda$  off an initial value

$$\Delta\lambda_{ij}^{\alpha\beta} = -\epsilon(\overline{x_i^\alpha x_j^\beta} - \langle x_i^\alpha x_j^\beta \rangle)$$

$$\Delta\lambda_i^\alpha = -\epsilon(\overline{x_i^\alpha} - \langle x_i^\alpha \rangle).$$

Here,  $\overline{x_i^\alpha x_j^\beta}$  and  $\overline{x_i^\alpha}$  represent the frequency counts of pairs and single amino acids, respectively, in the given sequence data set of interest; and  $\langle x_i^\alpha x_j^\beta \rangle$  and  $\langle x_i^\alpha \rangle$  represent the second and first order moments, respectively, calculated in the distribution defined by Eqns.(1) and (2).  $\epsilon$  is a small proportionality coefficient, which we set to 0.01. The  $\lambda$ 's are initialized with the  $\lambda_{ij}^{\alpha\beta}$  interaction terms set to zero, and the  $\lambda_i^\alpha$  terms chosen to match the single site probabilities of the given data. Further algorithmic and numerical details are given in the supplemental material [38].

- [26] N. Metropolis, A. Rosenbluth, M. Rosenbluth, A. Teller, E. Teller *J. Chem Phys.* **21** p. 1087 (1953)



[27] G. Hinton, T. Sejnowski, “Learning and Relearning in Boltzmann Machines” in *Parallel Distributed Processing*, eds. D. Rumelhart and J. McClelland MIT Press, Cambridge MA (1986)

[28] S. Lauritzen, *Graphical Models* Oxford Science Publications, Clarendon Press (1996)

[29] Pfam domains that were used follow, in format (Pfam name: Pdb designator, Pfam domain size, number of domain positions used, number of sequences)

(Ubiquitin family: 1ubi, domain size=82, length=76, number of sequences=555);

(Homeobox domain: 1fjl, domain size=57, length=57, number of sequences=1777);

(SH3 domain: 1shg, domain size=57, length=55, number of sequences=691);

(EF hand: 3icb, domain size=29, length=29, number of sequences=2159); (Ku-

nitz/Bovine pancreatic trypsin inhibitor domain: 6pti, domain size=51, length=51,

number of sequences=236;) (Ank repeat: 1awc, domain size=33, length=33, num-

ber of sequences=2220;) (Helix-loop-helix DNA-binding domain: 1mdy, domain

size=57, length=52, number of sequences=666) (SH2 domain: 1sha, domain size=79,

length=77, number of sequences=567); (4Fe-4S binding domain: 5fd1, domain

size=24, length=24, number of sequences=1209); (TPR domain: 1a17, domain

size=34, length=34, number of sequences=2507); (PDZ domain: 1be9, domain

size=83, length=81, number of sequences=721).

Sequence positions defining each folding domain were selected by using the “match state” positions of the associated Pfam Hidden Markov Model, available from the Pfam data base entry for each domain. “domain size” is the number of Pfam match states. Positions in a domain containing indels with less than fifty percent valid amino acids in the position were deleted from the domain definition. Positions in a domain containing indels, but with more than fifty percent valid amino acids in

the position, had the indels “filled in” with amino acids drawn randomly from the single site amino acid probability distribution for each such position. For simplicity, sequence weighting to attempt to address phylogenetic relatedness of sequences was not employed. Hennikoff sequence weighting was not found [18] to yield significant improvements, although conceivably other approaches might be fruitful.

[30] H. Berman, J. Westbrook, Z. Feng, G. Gilliland, T. Bhat H. Weissig, I. Shindyalov, P. Bourne, *Nuc. Acids. Res.* **28** pp. 235-242 (2000)

[31] N. Draper, H. Smith, *Applied Regression Analysis* second edition, Wiley, New York (1981)

[32] Linear partial correlation analysis has been applied to correlations of physico-chemical properties of amino acids within secondary structure elements, D. Afonnikov, Y. Kondrakhin, I. Titov, N. Kilchanov “Detecting Direct Correlations Between Positions in Multiple Alignments of Amino Acid Sequences” in Mewes, H.W. and Firsman, D. (eds) *Computer Science and Biology. Genome Informatics: Function, Structure, Phylogeny*, Proc. of the German Conference on Bioinformatics, pp. 87-98 (1997)

[33] The formula for conditional mutual information between site  $i$  and  $j$  is

$$CMI(i, j) = \sum_{x_i x_j X_r} P(x_i x_j X_r) \log \frac{P(x_i x_j | X_r)}{P(x_i | X_r) P(x_j | X_r)}$$

where  $x_i$  denotes the residue at  $i$ ,  $x_j$  the residue at  $j$ , and  $X_r$ , of length  $L-2$ , denotes the rest of the sequence of amino acids at all sites other than  $i$  and  $j$ .  $P(x_i x_j X_r)$  is merely the joint probability, Eqns. (1,2), of the complete  $L$  long sequence, while  $P(x_i x_j | X_r)$  is the conditional probability of a residue pair at  $i$  and  $j$ , given the rest of the  $L-2$  residues,  $X_r$ . Note that these probabilities are functions of the full set of  $\lambda$

parameters, i.e.,  $CMI(i, j)$  in contrast to  $MI(i, j)$ , involves interactions between all residues in the protein. The average of the *log* expression, above, can be accurately approximated by Monte Carlo importance sampling [26].

- [34] S. Saitoh, T. Nakai, K. Nishikawa, *Proteins* **15** pp. 191-204 (1993)
- [35] A. Ortiz, A. Kolinski, J. Skolnick, *J. Mol. Biol.* **277** ppp. 419-448 (1998)
- [36] This is closely related to specificity-sensitivity plots and the use of ROC curves for evaluating predictive power, see e.g. *Science* **240** pp 1285-93 (1988)
- [37] We thank Stefan Larson for provision of perl scripts that calculate the pairwise covariation measure in [18].
- [38] Supporting online material, to be available at a website, is presently included in the Appendix to this manuscript.
- [39] A. Horovitz, A. Fersht, *J. Mol. Biol.* **214** pp. 613-617 (1990)
- [40] When the  $\lambda_{ij}^{\alpha\beta}$  interaction terms are restricted to be zero, the remaining single site terms may be simply written in terms of the single site probabilities of the residues at each position in the sequence alignment:  $\lambda_i^\alpha = -\log[P(X_i^\alpha)]$ . Mutations to residues occurring more frequently in the alignment would thus be predicted to be stabilizing, an observation that is often found to be true in experiments, but with frequent exceptions. Allowing  $\lambda_{ij}^{\alpha\beta}$  to be nonzero addresses this and other co-operative effects of multiple mutations.
- [41] Q. Wang, A. Buckle, N. Foster, C. Johnson, A. Fersht, *Prot. Sci.* **8** pp. 2186-2193 (1999)
- [42] B. Kuhlman, D. Baker, *Proc. Natl. Acad. Sci. USA* **97** pp. 10383-10388 (2000)

- [43] D. Riddle, J. Santiago, S. Bray-Hall, N. Doshi, G. Grantcharova, Q. Yi, D. Baker, *Nature Str. Biol.* **4** pp. 805-809 (1997)
- [44] A. Keefe, J. Szostak, *Nature* **410** pp. 715-718 (2001)

The research of Lapedes and Jarzynski was supported by the Department of Energy under contract W-7405-ENG-36. The hospitality of the Santa Fe Institute where part of this work was performed is gratefully acknowledged. We thank Gary Stormo for very helpful feedback as these ideas evolved, and Steven Lockless, Rama Ranganathan, Stefan Larson and Tom Woolf for useful discussions.

## Appendix: Supporting Online Material

# 1 Determining the $\lambda$ Parameters by Maximum Likelihood Analysis

The maximum entropy probability distribution subject to constraints on the first and second order moments, has an exponential form

$$P(X) = \frac{\exp - [E(X)]}{Z},$$

where  $E$  is a sum of single and pairwise interactions,

$$E(X) = \sum_{\alpha\beta ij} \lambda_{ij}^{\alpha\beta} X_i^\alpha X_j^\beta + \sum_{\alpha i} \lambda_i^\alpha X_i^\alpha$$

and

$$Z = \sum_X \exp - [E(X)]$$

is a sum over all possible ( $20^L$ ) sequences of length  $L$  which normalizes the distribution [1].

The  $\lambda$ 's are Lagrange multipliers implementing the constraints that the first and second order moments of the distribution match the single and pairwise amino acid frequencies in a given sequence alignment. Each sequence  $X$  of the alignment may therefore be assigned a probability,  $P(X)$ , which is a function of the  $\lambda$ 's.

For each sequence alignment considered one may write the joint probability of all  $S$  sequences of the alignment as a function of the  $\lambda$ 's (assuming that the sequences are independent) as

$$P(\text{Sequences}) = \prod_{s=1}^{s=S} \frac{\exp - [E(X(s))]}{Z}$$

where  $s$  references each sequence of the alignment. Although naturally evolved sequences that are related by a phylogenetic tree are not independent, making the assumption of independence, for simplicity, still yields results of high accuracy (this assumption of

sequence independence is of course unrelated to issues of site independence within a sequence). Properly addressing the phylogenetic relatedness of sequences is complicated, but has the potential to increase accuracy still further.

Taking *logs* of both sides yields

$$\begin{aligned} \log[P(\text{Sequences})] &= -\left[ \sum_{\alpha\beta ijs} \lambda_{ij}^{\alpha\beta} X_i^\alpha(s) X_j^\beta(s) + \sum_{\alpha is} \lambda_i^\alpha X_i^\alpha(s) + S * \log(Z) \right] \\ &= -S * \left[ \sum_{\alpha\beta ij} \lambda_{ij}^{\alpha\beta} \overline{X_i^\alpha X_j^\beta} + \sum_{\alpha i} \lambda_i^\alpha * \overline{X_i^\alpha} + \log(Z) \right] \end{aligned}$$

Here,  $\overline{X_i^\alpha}$  and  $\overline{X_i^\alpha X_j^\beta}$  represent, respectively, the single and pairwise amino acid frequencies obtained by simple counting in the given aligned sequence data set.

A steepest ascent step, maximizing  $\log[P(\text{Sequences})]$ , changes the  $\lambda$  parameters by an amount proportional to the gradient of  $\log[P(\text{Sequences})]$  with respect to the  $\lambda$ 's

$$\begin{aligned} \Delta\lambda_{ij}^{\alpha\beta} &\sim \frac{\partial \log[P(\text{Sequences})]}{\partial \lambda_{ij}^{\alpha\beta}} \sim (\overline{X_i^\alpha X_j^\beta} - \langle X_i^\alpha X_j^\beta \rangle) \\ \Delta\lambda_i^\alpha &\sim \frac{\partial \log[P(\text{Sequences})]}{\partial \lambda_i^\alpha} \sim (\overline{X_i^\alpha} - \langle X_i^\alpha \rangle) \end{aligned}$$

where

$$\begin{aligned} \langle X_i^\alpha X_j^\beta \rangle &= -\frac{\partial \log(Z)}{\partial \lambda_{ij}^{\alpha\beta}} \\ \langle X_i^\alpha \rangle &= -\frac{\partial \log(Z)}{\partial \lambda_i^\alpha} \end{aligned}$$

represent the second and first order moments of the distribution, respectively. In principle, evaluating these moments involves  $(20^L)$  summations, however since they are simple averages they may be efficiently estimated in practice via Monte Carlo [2]. Once the moments have been estimated at a current setting of the  $\lambda$ 's, the  $\lambda$ 's are changed by an amount proportional to  $\Delta\lambda$  and the process is iterated to convergence. This procedure is essentially the ‘‘training’’ algorithm for a Boltzmann machine [3] when there are no hidden

units. Note that at the maximum of  $\log[P(\text{Sequences})]$ , i.e., when  $\Delta\lambda_{ij}^{\alpha\beta} = 0$ ,  $\Delta\lambda_i^\alpha = 0$ , the single and pairwise moments of the distribution match the single and pairwise amino acid frequencies of the given sequence alignment. Furthermore, it is possible to show by consideration of mixed second derivatives, such as  $\frac{\partial^2 \log[P(\text{Sequence})]}{\partial \lambda_{ij}^{\alpha\beta} \partial \lambda_{kl}^{\gamma\delta}}$ ,  $\frac{\partial^2 \log[P(\text{Sequence})]}{\partial \lambda_{ij}^{\alpha\beta} \partial \lambda_k^\gamma}$  that  $\log[P(\text{Sequence})]$  is a convex function and that there are no local maxima.

For the results reported in the main text, the  $\lambda$ 's were initialized with the  $\lambda_{ij}^{\alpha\beta}$  interaction terms set to zero, and the  $\lambda_i^\alpha$  terms chosen to match the single site amino acid frequencies of each given sequence alignment. To evaluate moments of the distribution given some current values of the  $\lambda$ 's, 400,000 sequence configurations were obtained by generating a Monte Carlo chain of 4,000,000 steps, and keeping every tenth configuration of this chain when estimating the  $\langle \rangle$  moments. Change in the  $\lambda$ 's,  $\Delta\lambda$ , are zero, and the iterative process converges, when the moments exactly match the amino acid frequencies. This occurs when the likelihood is a maximum and the gradient is zero. Effective convergence was reached in (very roughly) on the order of 10,000 – 15,000 changes of  $\Delta\lambda$ 's or 40 – 60 hours of computer time (depending on domain size), on a dedicated single processor 1 *ghz* cpu with 500 megbytes of memory. No significant effort was made to optimize code beyond addressing the most obvious inefficiencies.

## 2 Predicted Contacts for Eleven Families

The top 50 predicted contact pairs, using the Boltzmann network method (see main text), for each of the 11 Pfam families follows. Each column, representing one protein family, is ordered by descending value of conditional mutual information. The numbering scheme for specifying position pairs of each predicted contact uses the residue number appearing on the “ATOM” lines in the PDB files listed at the top of each column.

<i>1ubi</i>	<i>1fjl</i>	<i>1shg</i>	<i>3icb</i>	<i>6pti</i>	<i>1awc</i>	<i>1mdy</i>	<i>1sha</i>	<i>5fd1</i>	<i>1a17</i>	<i>1be9</i>
19, 24	6, 13	44, 53	56, 58	20, 44	72, 101	139, 141	6, 33	24, 25	34, 50	367, 375
19, 57	24, 29	31, 44	50, 66	24, 31	79, 82	125, 135	18, 31	3, 4	43, 46	329, 33
24, 57	3, 7	25, 31	49, 50	13, 36	94, 95	129, 155	56, 80	4, 7	35, 51	336, 37
20, 22	17, 52	31, 53	49, 66	21, 48	91, 97	136, 148	33, 86	12, 17	31, 50	353, 39
28, 57	6, 7	53, 58	45, 70	21, 31	96, 98	120, 125	65, 86	17, 18	53, 56	366, 36
16, 22	28, 30	17, 24	58, 60	7, 42	80, 101	119, 149	79, 82	7, 10	34, 38	346, 35
20, 25	29, 43	21, 22	50, 53	27, 52	77, 81	141, 161	56, 84	6, 7	32, 36	319, 32
23, 26	2, 7	25, 53	63, 66	14, 38	72, 80	125, 151	11, 45	5, 22	46, 49	316, 35
19, 25	27, 29	35, 43	50, 52	9, 16	82, 83	123, 129	10, 14	1, 7	42, 44	350, 35
20, 26	24, 45	15, 55	46, 58	48, 52	79, 80	125, 148	80, 84	1, 10	29, 33	325, 37
23, 31	29, 36	42, 55	58, 67	23, 54	77, 80	135, 155	6, 28	22, 23	38, 46	366, 36
16, 24	31, 55	15, 21	48, 70	21, 52	80, 83	151, 153	31, 84	13, 18	33, 36	323, 36
22, 24	8, 43	44, 58	62, 63	27, 54	81, 83	124, 136	7, 28	7, 18	58, 61	338, 35
19, 20	27, 30	14, 26	50, 70	44, 52	97, 98	116, 131	59, 60	1, 4	36, 51	323, 37
23, 25	10, 13	15, 42	69, 70	15, 21	80, 81	129, 145	14, 61	3, 10	39, 51	322, 38
24, 28	28, 34	9, 33	45, 73	8, 25	79, 87	125, 147	42, 46	5, 9	58, 60	335, 33
20, 24	21, 24	13, 57	60, 62	27, 48	88, 92	123, 125	49, 86	1, 26	59, 61	341, 35
19, 28	23, 27	24, 25	58, 64	22, 31	83, 86	147, 161	84, 85	1, 22	38, 43	369, 37
16, 18	28, 33	13, 56	66, 67	46, 48	99, 101	139, 142	79, 86	5, 7	41, 43	338, 34
16, 56	8, 58	33, 39	53, 69	36, 39	81, 87	152, 154	6, 10	10, 13	37, 40	358, 39
16, 20	34, 39	25, 52	49, 53	16, 34	89, 93	110, 114	31, 33	9, 13	33, 51	330, 371
26, 28	29, 45	10, 29	63, 67	23, 24	83, 87	116, 124	28, 80	2, 22	37, 41	345, 350
25, 54	33, 34	17, 33	53, 66	22, 53	72, 86	120, 136	6, 55	5, 26	35, 50	316, 325
22, 56	30, 43	17, 34	53, 63	21, 24	77, 101	122, 125	14, 43	1, 3	32, 33	367, 370
3, 18	15, 45	12, 13	46, 47	7, 11	79, 97	145, 157	10, 36	1, 2	39, 44	323, 346
54, 64	36, 39	34, 45	46, 67	17, 36	72, 77	136, 140	36, 79	2, 4	58, 59	314, 325
25, 26	4, 7	35, 37	62, 69	16, 36	77, 83	113, 116	28, 46	10, 22	48, 52	314, 338
20, 54	21, 34	7, 36	62, 67	9, 34	72, 82	131, 141	25, 28	2, 18	29, 30	361, 367
18, 22	28, 54	39, 52	58, 72	6, 23	93, 101	113, 136	10, 78	5, 10	54, 57	322, 327
12, 25	29, 39	10, 59	57, 70	10, 13	72, 83	153, 157	10, 28	10, 26	30, 36	362, 376
23, 28	7, 10	38, 52	56, 57	8, 26	85, 88	116, 138	7, 10	17, 25	28, 61	329, 371
3, 16	15, 17	22, 52	46, 72	8, 46	97, 101	144, 152	9, 33	19, 22	28, 32	379, 380
19, 54	29, 34	10, 52	50, 63	27, 31	97, 100	124, 145	9, 11	3, 5	38, 50	330, 372
12, 20	23, 34	33, 37	45, 48	23, 26	86, 87	147, 152	78, 82	4, 5	32, 51	367, 378
16, 57	7, 41	31, 52	58, 62	29, 49	77, 97	114, 122	14, 74	7, 13	28, 54	337, 382
19, 22	7, 13	12, 39	56, 61	44, 46	77, 82	134, 138	61, 74	1, 23	33, 37	372, 376
60, 64	34, 45	22, 53	56, 62	28, 29	70, 80	128, 133	41, 82	1, 13	33, 61	325, 337
23, 39	41, 43	9, 60	49, 73	8, 16	93, 100	148, 151	47, 61	1, 5	32, 61	362, 386
22, 25	8, 14	33, 34	46, 53	6, 28	79, 81	136, 159	11, 46	2, 13	48, 57	322, 345
54, 60	26, 44	10, 30	49, 52	15, 36	70, 72	125, 154	36, 41	5, 13	50, 53	341, 348
20, 23	32, 36	9, 18	66, 73	16, 28	87, 89	110, 149	11, 59	4, 6	31, 53	354, 388
23, 32	26, 46	9, 17	67, 71	10, 42	80, 97	136, 151	31, 40	6, 10	32, 55	314, 350
25, 28	2, 33	11, 25	53, 70	21, 39	70, 85	113, 120	10, 60	24, 26	30, 33	361, 375
18, 26	24, 39	24, 57	49, 61	31, 48	74, 80	116, 127	37, 41	25, 26	49, 53	345, 346
16, 26	4, 6	9, 42	52, 70	21, 22	82, 84	148, 154	73, 75	13, 19	28, 30	341, 359



### 3 A Computational Survey of ( $20^3$ ) Mutants of the Hydrophobic Core of Fyn SH3

The high correlation reported in the main text for calculated  $\Delta G$  values with measured melting temperatures, for mutations in positions 26, 39 and 50 (numbering scheme of reference [4]), suggests performing a computational survey of all ( $20^3$ ) possible mutants in these positions. Using the regression line of Fig. (3) of the main text enables conversion of any calculated  $\Delta G$  to a predicted melting temperature. We surveyed all ( $20^3$ ) possible mutants in these three positions and selected those mutant sequences with predicted melting temperatures within the range of measured melting temperatures of Fig.(3), in effect interpolating new sequences between existing sequences with measured melting temperatures. Regarding sequences outside of this range: sequences with significantly higher melting temperatures were not found; on the other end of the temperature range, sequences utilizing amino acids that were rare in the initial sequence alignment depend on  $\lambda$  parameters that are poorly determined, and were eliminated from the set of significant predictions. 50 such triple mutants, ordered by predicted melting temperature, are listed below. The numbering scheme is that of reference [4]: residues listed correspond to positions 4,6,10,18,20,26,28,37,39,50,55.

<i>Sequence</i>	<i>Temperature</i>
<i>FAYLFLIWAIV</i>	84.9
<i>FAYLFFIWAIV</i>	78.7
<i>FAYLFIIWAIV</i>	71.6
<i>FAYLFIIWGFV</i>	69.8
<i>FAYLFIIWGIV</i>	69.6
<i>FAYLFLIWAIV</i>	69.3
<i>FAYLFMIWAIV</i>	69.2
<i>FAYLFLIWGIV</i>	67.7
<i>FAYLFFIWGIV</i>	64.7
<i>FAYLFLI WVIV</i>	63.5
<i>FAYLFFIWAIV</i>	60.8
<i>FAYLFLIWCIV</i>	60.7
<i>FAYLFFI WVIV</i>	60.1
<i>FAYLFLI WALV</i>	59.6
<i>FAYLFIIWGVV</i>	58.0
<i>FAYLFIIWGLV</i>	57.8
<i>FAYLFCIWAIV</i>	57.6
<i>FAYLFIIWAIV</i>	57.3
<i>FAYLFLI WAFV</i>	56.6
<i>FAYLFMIWGIV</i>	56.3
<i>FAYLFFIWCIV</i>	56.3
<i>FAYLFLI WIIV</i>	56.0
<i>FAYLFLI WGFV</i>	55.7
<i>FAYLFII WAFV</i>	55.3
<i>FAYLFII WVIV</i>	55.0
<i>FAYLFLI WGVV</i>	54.8
<i>FAYLFLI WVVV</i>	54.7
<i>FAYLFFI WGFV</i>	54.7
<i>FAYLFLI WAYV</i>	54.7
<i>FAYLFMI WAIV</i>	54.5
<i>FAYLFLI WAAV</i>	54.1
<i>FAYLFFI WALV</i>	54.1
<i>FAYLFIIWCIV</i>	53.2
<i>FAYLFII WALV</i>	52.8
<i>FAYLFII WGYV</i>	52.8
<i>FAYLFAIWAIV</i>	52.7
<i>FAYLFFI WIIV</i>	52.4
<i>FAYLFFI WAFV</i>	52.3
<i>FAYLFLI WCVV</i>	52.0
<i>FAYLFMI WVIV</i>	50.7
<i>FAYLFII WGAV</i>	50.7
<i>FAYLFII WIIV</i>	49.6
<i>FAYLFSIWAIV</i>	49.6
<i>FAYLFFI WGVV</i>	49.5
<i>FAYLFMIWCIV</i>	49.5
<i>FAYLFLI WGLV</i>	49.4
<i>FAYLFFI WVVV</i>	49.0
<i>FAYLFFI WAYV</i>	48.8
<i>FAYLFMI WCEV</i>	48.2

## 4 A Computational Survey of $(20^{11})$ Hydrophobic Core Sequences of Fyn SH3

A computational survey of sequence space can also be performed using the Boltzmann network formalism, even when the number of potential sequences in the survey precludes exhaustive enumeration. We illustrate this by suggesting complete redesigns for the eleven residue hydrophobic core sequence of SH3, for which an exhaustive survey of  $(20^{11})$  possible core sequences is infeasible. A stochastic search via simulated annealing, using the modified Lam schedule for temperature changes [5,6], was used to compile a list of the 50 most stable sequences identified during the annealing process. Of these predicted core sequences, 26 occur in the initial sequence alignment, i.e. occur in naturally evolved proteins, and constitute predictions of the melting temperatures of these natural sequences. The remaining 24 sequences constitute predictions of new stable core sequences. Residues listed below correspond to positions 4,6,10,18,20,26,28,37,39,50,55 in the numbering scheme of reference [4].

<i>Sequence</i>	<i>Temperature</i>
<i>FAYLFLIWAIV</i>	84.9
<i>VAYLFIVWGFV</i>	84.6
<i>VAYLFLIWAIV</i>	79.3
<i>VAYLFLVWAIV</i>	79.0
<i>FAYLFFIWAIV</i>	78.7
<i>AAYLFIVWGFV</i>	77.6
<i>VAF LFIVWGFV</i>	77.3
<i>FAYLFLVWAIV</i>	76.8
<i>VAYLFIIWGFV</i>	76.7
<i>VAYLFILWGFV</i>	76.3
<i>FAFLFLIWAIV</i>	76.3
<i>AAFLFIIWGFV</i>	76.0
<i>AAYLFIIWGFV</i>	75.9
<i>VAYLLIVWGFV</i>	75.7
<i>YAYLFIVWGFV</i>	75.4
<i>VAYLFINWGFV</i>	75.4
<i>AAFLFIVWGFV</i>	75.2
<i>AAYLFLIWAIV</i>	74.0
<i>AAFLFIVYGFV</i>	73.6
<i>VAYLFIVLGFV</i>	73.3
<i>VAYIFIVWGFV</i>	73.1
<i>VAYLFIVWGIV</i>	72.8
<i>AAFLFIIYGFV</i>	72.7
<i>VAYLFIVYGFV</i>	72.6
<i>VAYLLVWGFV</i>	72.3
<i>VAYLFIIWGIV</i>	72.0
<i>VAF LFIIWAIV</i>	71.9
<i>VAF LFIIWGFV</i>	71.9
<i>VAF LFIVYGFV</i>	71.8
<i>FAYLFIIWAIV</i>	71.6
<i>AAYLFINWGFV</i>	71.5
<i>AAFLFLIWAIV</i>	71.5
<i>VAF LFILWGFV</i>	71.5
<i>AAFLFILWGFV</i>	71.3
<i>AAYLFILWGFV</i>	71.3
<i>FAYLFLIWAII</i>	71.0
<i>AAFLFIIYGFV</i>	71.0
<i>VAYLFFIWAIV</i>	71.0
<i>VAYLFLVWGIV</i>	70.8
<i>VAYLFLVWGFV</i>	70.4
<i>CAYLFIVWGFV</i>	70.2
<i>VAYLFVVWGFV</i>	70.2
<i>AAYLLIVWGFV</i>	70.2
<i>FAYLFLIWAII</i>	70.1
<i>AAFLIIWGFV</i>	70.0
<i>CAYLFLIWAIV</i>	69.9
<i>FAYLFIVWGFV</i>	69.9
<i>FAYLFIIWGFV</i>	69.8
<i>VAYLIIYVIGFV</i>	69.8

### Supplemental Material References

- [1] A. Lapedes, B. Giraud, L. Liu, G. Stormo, “Correlated Mutations In Models of Protein Sequences: Phylogenetic and Structural Effects”, *Proceedings of the IMS/AMS 1997 International Conference on Statistics in Computational Molecular Biology (Seattle 1997)*, published as Vol 33, Monograph Series of the Inst. for Mathematical Statistics (Hayward Press )
- [2] N. Metropolis, A. Rosenbluth, M. Rosenbluth, A. Teller, E. Teller, *J. Chem Phys.* **21** p. 1087 (1953)
- [3] G. Hinton, T. Sejnowski, “Learning and Relearning in Boltzmann Machines” in *Parallel Distributed Processing*, eds. D. Rumelhart, J. McClelland MIT Press, Cambridge MA (1986)
- [4] S. Larson, A. Di Nardo, A. Davidson, *J. Mol. Biol.* **303** pp. 433-446 (2000)
- [5] J.Lam, J. Delosme “Performance of a New Annealing Schedule”, in *Proc. of the 25<sup>th</sup> ACM/IEEE Design Automation Conference*, pp. 306-311, IEEE Computer Society Press (1988)
- [6] W. Swartz, C. Sechen “New Algorithms for the Placement and Routing of Macro Cells”, in *Proc. of the IEEE Intl. Conference on Computer Aided Design*, pp. 336-339, IEEE Computer Society Press (1990)